Early programming of CD8+ T cell response by the orphan nuclear receptor NR4A3

Livia Odagiu[a,b], Salix Boulet[a], Dave Maurice De Sousa[a,b], Jean-François Daudelin[a], Sandrine Nicolas[a], and Nathalie Labrecque[a,b,c,1]

[a]Laboratory of Immunology, Maisonneuve-Rosemont Hospital Research Center, Montreal, QC H1T 2M4, Canada; [b]Département de Microbiologie, Infectiologie et Immunologie, Université de Montréal, Montreal, QC H3C 3J7, Canada; and [c]Département de Médecine, Université de Montréal, Montreal, QC H3C 3J7, Canada

Enhancing long-term persistence while simultaneously potentiating the effector response of CD8+ T cells has been a long-standing goal in immunology to produce better vaccines and adoptive cell therapy products. NR4A3 is a transcription factor of the orphan nuclear receptor family. While it is rapidly and transiently expressed following T cell activation, its role in the early stages of T cell response is unknown. We show that NR4A3-deficient murine CD8+ T cells differentiate preferentially into memory precursor and central memory cells, but also produce more cytokines. This is explained by an early influence of NR4A3 deficiency on the memory transcriptional program and on accessibility of chromatin regions with motifs for bZIP transcription factors, which impacts the transcription of Fos/Jun target genes. Our results reveal a unique and early role for NR4A3 in programming CD8+ T cell differentiation and function. Manipulating NR4A3 activity may represent a promising strategy to improve vaccination and T cell therapy.

early CD8+ T cell response | nuclear receptors | T cell memory | NR4A3 | T cell function

CD8+ T lymphocytes undergo massive expansion and differentiation following T cell receptor (TCR) recognition of foreign antigens presented as peptide fragments on MHC class I molecules. At the peak of the CD8+ T cell response to acute infection, two main populations of effectors are generated: short-lived effector cells (SLECs; KLRG1hiCD127lo) and memory precursor effector cells (MPECs; KLRG1loCD127hi) (1–3). Both populations have effector functions but most of the SLECs will die during the contraction phase while MPECs will further differentiate into long-lived CD8+ memory T cells to confer long-term protection. The SLEC and MPEC differentiation choice is influenced by inflammatory signals perceived by the T cells and requires the induction of a complex transcriptional program (2, 3). As such, several transcription factors were shown to contribute to this differentiation event. SLEC differentiation is dependent on T-bet, Blimp-1, Id2, Rbpjk, and Zeb2 while Eomes, Bcl-6, Id3, Bach2, and TCF-1 are involved in MPEC and memory T cell differentiation (2, 4–15). Evidence supports that this differentiation choice is determined very early in the response, as early as the first T cell division (16). Furthermore, the chromatin landscape changes rapidly following naive CD8+ T cell activation with massive opening of chromatin regions. Interestingly, the differentially accessible regions (DARs) of chromatin between naive and recently activated CD8+ T cells contain regions that are later preferentially found in either MPECs or SLECs (17–19). This suggests that early events of T cell activation poise the cells for differentiation and that further events fix the cellular differentiation choice. The DARs associated with early CD8+ T cell activation are enriched for motifs recognized by several transcription factors, including some that are known to influence CD8+ T cell differentiation (17–19).

Among early events that occur following TCR stimulation of naive CD8+ T cells is the rapid expression of the nuclear orphan receptor NR4A family members (NR4A1, NR4A2, and NR4A3)

(20). These orphan nuclear receptors act as transcription factors by binding to the NBRE consensus sequence motif on DNA (reviewed in ref. 21). Their activity is regulated at the level of their expression and they are induced very rapidly by a variety of extracellular signals. They are thus considered immediate early genes. They control proliferation, differentiation, survival, and metabolism in several cell types (21). In the immune system, they play crucial roles in the differentiation and response of myeloid cells (22–26). In T cells, the deletion of the three members during thymocyte differentiation abrogates regulatory T cell differentiation while single deletion results in an increase in these cells (27–29). Their roles in the peripheral mature T cell compartment have not been extensively studied but NR4As are highly expressed by exhausted T cells (30–34) and recent studies have found roles for these in contexts of recurrent antigen stimulation (33, 35). However, very little is known about the role of these members during CD8+ T cell response to acute infection and on the specific action of NR4A3 in CD8+ T cells. The rapid and transient up-regulation of NR4A1-3 expression following CD8+ T cell activation suggests that these transcription factors will have an early transcriptional influence on CD8+ T cell response to acute infection. This possibility is further supported by the enrichment of the NBRE motif in DARs that are more open at 2 to 24 h postnaive CD8+ T cell activation while they are not enriched in more differentiated effector CD8+ T cells (17–19).

Significance

The CD8+ T cell response is crucial in protecting the organism against infections and cancer. This protective response relies on the production of effector molecules and the generation of long-lived memory cells. Understanding the processes governing CD8+ T cell responses is essential for the development of better vaccine strategies and immune cell therapies. Here, we show that deletion of the transcription factor NR4A3 leads to increased memory generation and effector functions. This results from an early impact on the CD8+ T cell transcriptional memory program and on chromatin accessibility for bZIP transcription factors. Thus, we identify NR4A3 as a key regulator of CD8+ T cell function and differentiation, which could have therapeutic implications.

In this study, we have found an important and unique role for NR4A3 in the early stages of an acute CD8$^+$ T cell response. We demonstrate that NR4A3 limits the generation of MPECs and memory CD8$^+$ T cells, particularly central memory CD8$^+$ T cells, while restraining cytokine production. Early in the CD8$^+$ T cell response, NR4A3 decreases chromatin accessibility of regions containing bZIP transcription factor motifs and reduces the expression of transcription factors involved in memory differentiation while enhancing expression of transcription factors controlling SLEC differentiation. This highlights the crucial early role for the NR4A3 family member in acute CD8$^+$ T cell responses.

Results

NR4A3 Deficiency Promotes MPEC Differentiation and Enhances Effector Functions.
To evaluate the intrinsic role of NR4A3 during CD8$^+$ T cell response, we crossed $Nr4a3^{-/-}$ mice with OT-I mice, expressing a transgenic TCR specific for the ovalbumin (OVA) peptide 257 to 264 in the context of the MHC class I molecules K^b (36). A total of 5×10^3 $Nr4a3^{+/+}$ or $Nr4a3^{-/-}$ OT-I T cells were adoptively transferred into wild-type (WT) congenic B6.SJL mice 1 d prior to infection with a subthetal dose of *Listeria monocytogenes* encoding OVA (Lm-OVA). As shown in Fig. 1*A*, NR4A3 deficiency did not affect CD8$^+$ T cell expansion at the peak of the response (day 7) or the kinetic of the CD8$^+$ T cell response (*SI Appendix*, Fig. S1*A*). We did, however, consistently observe the generation of twofold more memory CD8$^+$ T cells in the absence of NR4A3 (Fig. 1*A* and *SI Appendix*, Fig. S1*A*). This increased memory generation was also observed following lymphocytic choriomeningitis virus encoding OVA (LCMV-OVA) infection when OT-I $Nr4a3^{-/-}$ T cells were adoptively transferred in competition with $Nr4a3^{+/+}$ OT-I T cells (*SI Appendix*, Fig. S1*B*). The enhanced generation of memory CD8$^+$ T cells in absence of NR4A3 led us to evaluate whether the proportion of SLECs and MPECs was affected. At day 7 postinfection, we observed an increased proportion of MPECs while fewer SLECs were present in the spleen (Fig. 1*B*) and blood (*SI Appendix*, Fig. S1*C*). Similar effects on MPEC/SLEC differentiation were obtained following dendritic cell vaccination, LCMV-OVA infection, and polyclonal CD8$^+$ T cell response (*SI Appendix*, Fig. S1 *D–F*). Although, we did not observe differences in thymic differentiation and peripheral OT-I T cells (*SI Appendix*, Fig. S2 *A–E*), we confirmed our results using sorted CD44^{lo} naive OT-I T cells (*SI Appendix*, Fig. S2*F*). Finally, to test whether overexpression of NR4A3 promoted the generation of SLECs, we stimulated $Nr4a3^{+/+}$ and $Nr4a3^{-/-}$ OT-I CD8$^+$ T cells with OVA-pulsed splenocytes in vitro for 24 h, spin transduced them with defective retrovirus encoding $Nr4a3$, and adoptively transferred the transduced OT-I cells into B6.SJL mice infected with Lm-OVA the day before. As shown in Fig. 1*C*, overexpression of NR4A3 in $Nr4a3^{+/+}$ or $Nr4a3^{-/-}$ OT-I T cells led to increased SLEC differentiation while MPEC generation was decreased. Therefore, NR4A3 modulates the generation of CD8$^+$ memory T cells by influencing the generation of MPECs at the peak of the CD8$^+$ T cell response.

The generation of fewer SLECs in absence of NR4A3 raises the possibility that effectors are less differentiated and as such might be less functional. However, after a short in vitro restimulation with the OVA peptide, more $Nr4a3^{-/-}$ effectors produced cytokines (IFN-γ, TNF-α, and IL-2) than their WT counterpart and they produced them in higher amounts (Fig. 2*A*). The effect of NR4A3 deficiency on cytokine production was also observed in the polyclonal T cell repertoire setting (*SI Appendix*, Fig. S3*A*). This enhanced cytokine production is observed in both MPECs and SLECs (*SI Appendix*, Fig. S3*B*). Overexpression of NR4A3 in $Nr4a3^{+/+}$ and $Nr4a3^{-/-}$ OT-I T cells led to a reduction of cytokine production (Fig. 2*B*). Therefore, NR4A3 deficiency promotes both memory generation

and functional capacity of CD8$^+$ T cells, two processes that are usually not coregulated.

NR4A3 Deficiency Promotes the Differentiation of Central Memory CD8$^+$ T Cells.
To test whether enhanced memory generation was a consequence of an increased proportion of MPECs at the peak of the T cell response, we sorted $Nr4a3^{+/+}$ and $Nr4a3^{-/-}$ OT-I MPECs from the spleen of mice infected with Lm-OVA (day 5) and adoptively transferred the same numbers in competition in WT recipients (Fig. 3*A*). The rate of memory generation from $Nr4a3^{+/+}$ and $Nr4a3^{-/-}$ MPECs was slightly higher for NR4A3-deficient MPECs, indicating that increased memory CD8$^+$ T cell generation was the consequence of both an increased MPEC generation and enhanced differentiation into memory T cells (Fig. 3*A*). Greater differentiation of MPECs into long-lived memory CD8$^+$ T cells is probably not the consequence of improved survival during the contraction phase but may result from enhanced sensitivity of $Nr4a3^{-/-}$ OT-I memory T cells to IL-15 (*SI Appendix*, Fig. S4 *A* and *B*).

The characterization of CD8$^+$ memory T cell generation shows that the number of memory CD8$^+$ T cells is increased in the spleen (Fig. 1*A*), lymph nodes, and bone marrow in the absence of NR4A3 (Fig. 3*B*) with a higher proportion of cells bearing a CD62L^{hi} central memory phenotype (Fig. 3*C*). As a consequence, a greater proportion of $Nr4a3^{-/-}$ OT-I CD8$^+$ memory T cells coproduce IL-2 and IFN-γ (Fig. 3*D*). Similar results were obtained using LCMV-OVA infection in a competitive setting (*SI Appendix*, Fig. S4 *C* and *D*). Finally, we did not observe any differences in homeostatic proliferation of $Nr4a3^{+/+}$ and $Nr4a3^{-/-}$ OT-I memory T cells (*SI Appendix*, Fig. S4 *E* and *F*)

Following adoptive transfer and challenge with a high dose of Lm-OVA, $Nr4a3^{-/-}$ OT-I memory T cells expand as efficiently as $Nr4a3^{+/+}$ OT-I memory cells (Fig. 3 *E* and *F*) and the generated secondary CD8$^+$ T effectors were still more polyfunctional after rechallenge (Fig. 3*G*) and differentiate more into MPECs and CD62L^{hi} cells (*SI Appendix*, Fig. S4*G*). To analyze the capacity of $Nr4a3^{+/+}$ and $Nr4a3^{-/-}$ OT-I memory T cells to control a bacterial challenge, we generated OT-I memory CD8$^+$ T cells following LCMV-OVA infection and challenge the recipient mice with 5×10^5 colony-forming units (CFUs) of Lm-OVA. We did not observe a better control of bacterial burdens in mice containing $Nr4a3^{-/-}$ OT-I memory T cells (*SI Appendix*, Fig. S4*H*). This might be the consequence of a very potent control of bacteria in the WT setting or may reflect a lack of better control of Lm-OVA by central memory T cells. The enrichment for memory T cells with a central memory phenotype and the enhanced functionality of $Nr4a3^{-/-}$ CD8$^+$ T cells led us to evaluate whether they would better control tumor growth. To do so, 2×10^5 $Nr4a3^{+/+}$ or $Nr4a3^{-/-}$ memory OT-I T cells generated following Lm-OVA infection were adoptively transferred into mice bearing B16-OVA melanomas. In this setting, only NR4A3-deficient memory CD8$^+$ T cells were able to provide prolonged mice survival and reduced tumor growth (Fig. 3*H* and *SI Appendix*, Fig. S4*I*). Therefore, NR4A3 deficiency favors the generation of more central memory CD8$^+$ T cells that are endowed with enhanced functions and ability to control tumor growth.

NR4A3 Deficiency Influences Early Expression of Transcription Factors Important for MPEC and Memory CD8$^+$ T Cell Generation.
To understand how NR4A3 deficiency promotes enhanced MPEC and memory CD8$^+$ T cell generation while at the same time enhancing effector functions, we performed the analysis of the transcriptome of $Nr4a3^{+/+}$ and $Nr4a3^{-/-}$ OT-I T cells early after in vivo T cell activation, before MPEC/SLEC differentiation (*SI Appendix*, Fig. S5*A*), as $Nr4a3$ expression is induced early and transiently following T cell stimulation in vivo (peak at 24 h
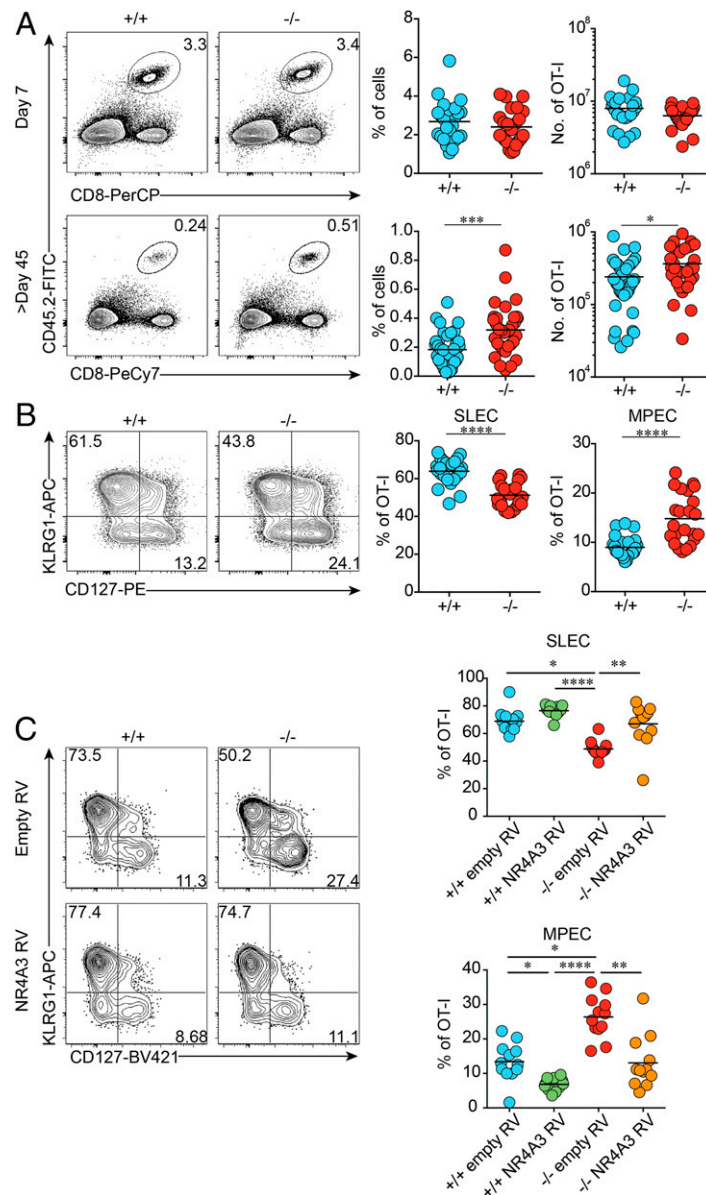
Fig. 1. NR4A3 restrains CD8+ T cell memory generation. (*A*) Effector and memory responses in the spleen of mice adoptively transferred with CD45.2+ *Nr4a3*+/+ or *Nr4a3*−/− OT-I cells prior to Lm-OVA infection. (*B*) Proportions of MPECs (CD127+KLRG1−) and SLECs (CD127−KLRG1+) within OT-I effectors at day 7 postinfection. (*C*) *Nr4a3*+/+ and *Nr4a3*−/− OT-I cells transduced with empty- or *Nr4a3*-encoding retrovirus (RV) were transferred into Lm-OVA-infected mice. At day 7 postinfection, MPEC and SLEC distribution in GFP+-transduced cells was evaluated. +/+: *Nr4a3*+/+ cells; −/−: *Nr4a3*−/− cells. Each dot represents one mouse. Data are from at least three independent experiments. Unpaired Student's *t* test, with a Welch's correction when applied, was used for two-group comparison and Kruskal–Wallis ANOVA with Dunn's multiple comparison for multiple group comparison: *$P < 0.05$, **$P < 0.01$, ***$P < 0.001$, ****$P < 0.0001$.

postinfection with Lm-OVA; *SI Appendix*, Fig. S5*B*). At early time points, day 2 and day 3 postinfection, we did not observe any defect in proliferation and acquisition of the activation markers CD69 and CD44 by *Nr4a3*+/+ and *Nr4a3*−/− OT-I T cells (*SI Appendix*, Fig. S5 *C* and *D*) further validating the choice of day 3 for the RNA sequencing (RNA-seq) analysis. At day 3 postinfection with Lm-OVA, 355 genes were differentially expressed in *Nr4a3*+/+ and *Nr4a3*−/− OT-I T cells (fold change [FC] >|1.5| and *P* adjusted [adj] <0.05), among them 274 genes show higher expression in absence of NR4A3 while 81 genes were down-regulated (Fig. 4*A* and Dataset S1). Gene set enrichment analysis (GSEA) showed enrichment for several gene signatures associated with immune memory (Fig. 4*B*). In agreement with this, at day 3 of the response, the expression of transcription factors controlling MPEC and memory generation

(*Tcf7*, *Eomes*, *Id3*, *Bcl6*, and *Bach2*) was increased while the expression of many transcription factors controlling SLEC differentiation (*Id2*, *Prdm1*, *Zeb2*, and *Rbpj*) was down-regulated in the absence of NR4A3 (Fig. 4*C*). We validated by fluorescence-activated cell sorting (FACS) and RT-qPCR analysis that the expression of these transcription factors was modulated by NR4A3 in OT-I effector T cells at day 3 postinfection with Lm-OVA (*SI Appendix*, Fig. S5 *E* and *F*) and the changes in the expression of these transcription factors were maintained in day-7 effectors (Fig. 4 *D* and *E*), except for T-bet. Our data also reveal a role for NR4A3 in promoting SLEC differentiation via the regulation of the *Il2ra* gene (37, 38). *Il2ra* gene transcription and CD25 protein expression are significantly down-regulated in day-3 *Nr4a3*−/− OT-I effector T cells (Fig. 4 *A*, *F*, and *G*). Moreover, *Nr4a3*−/− OT-I T cells at day 3 postinfection are
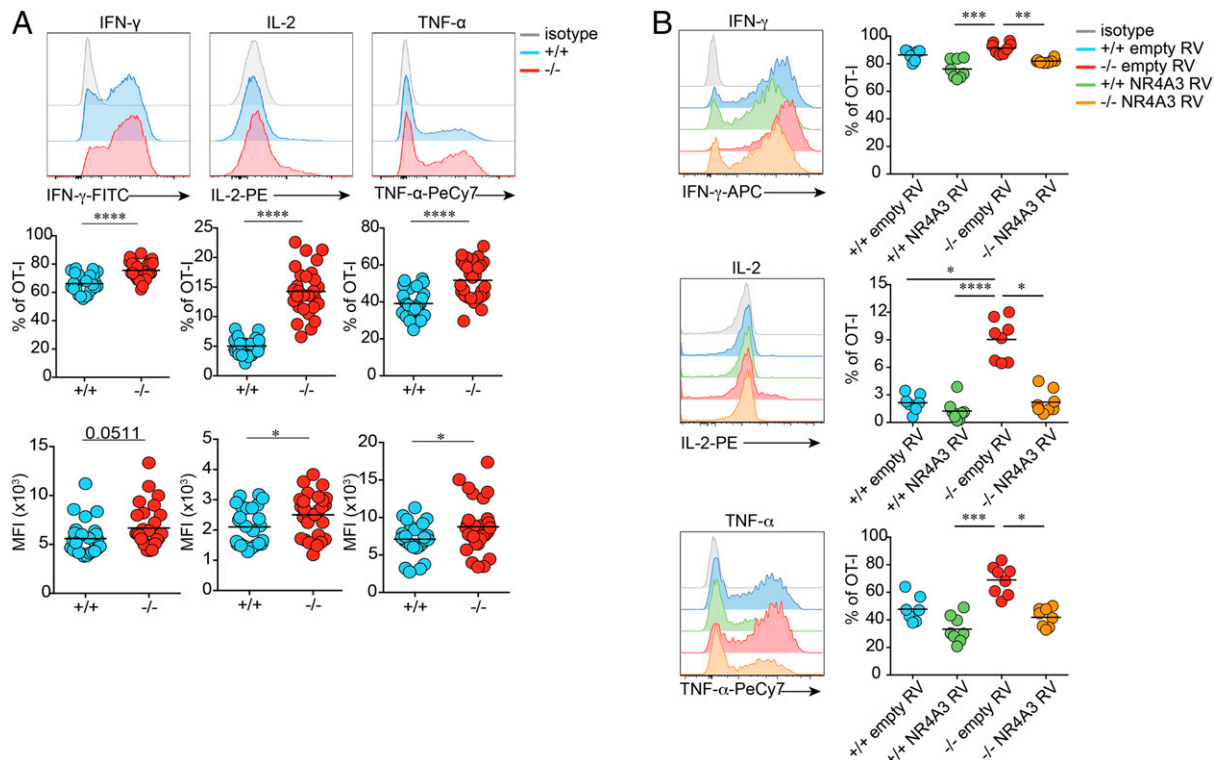
Fig. 2. NR4A3 restrains cytokine production by CD8$^+$ T cells. (*A*) Day 7 postinfection with Lm-OVA, OT-I effectors were restimulated for 5 h with OVA peptide and assessed for cytokine secretion. The percentage of positive OT-I cells for each cytokine and mean fluorescence intensity (MFI) on cells positive for the measured cytokines are shown. (*B*) Retrovirally transduced GFP$^+$ cells, as in Fig. 1*C*, were sorted prior to restimulation in order to measure cytokine production. $^{+/+}$: *Nr4a3*$^{+/+}$ cells; $^{-/-}$: *Nr4a3*$^{-/-}$ cells. Data are from two (*B*) or at least three independent experiments. Unpaired Student's *t* test, with a Welch's correction when applied, was used for two-group comparison and Kruskal–Wallis ANOVA with Dunn's multiple comparison for multiple group comparison: *$P < 0.05$, **$P < 0.01$, ***$P < 0.001$, ****$P < 0.0001$.

enriched for the CD25^{lo}CD62L^{hi} subset when compared to *Nr4a3*$^{+/+}$ OT-I T cells (*SI Appendix*, Fig. S5*G*), a subset identified by others to be committed to differentiate into memory cells (39), further supporting the idea that NR4A3 deficiency has an early impact on the acquisition of the memory program. Altogether, these data show that NR4A3 deficiency has an immediate impact on the central molecular events that regulate CD8$^+$ T cell fate.

NR4A3 Influences Chromatin Accessibility Early during T Cell Activation. As NR4A3 is rapidly and transiently induced in antigen-stimulated CD8$^+$ T cells and because it has an early impact on the programming of effector differentiation, we decided to determine the effect of NR4A3 deficiency on chromatin accessibility using assay for transposase-accessible chromatin sequencing (ATAC-seq). To do so, we first validated that *Nr4a3*$^{-/-}$ OT-I T cells stimulated in vitro for 3 d showed similar changes in expression of selected transcription factors and enhanced cytokine production (*SI Appendix*, Fig. S6*A*). In this in vitro setting, *Nr4a3* transcription peaks at 12 h poststimulation (*SI Appendix*, Fig. S6*B*). Therefore, we extracted nuclei from *Nr4a3*$^{+/+}$ and *Nr4a3*$^{-/-}$ OT-I T cells stimulated for 12 h to perform the ATAC-seq. As shown in Fig. 5*A* and Dataset S2, a total of 1,572 DARs of chromatin were identified (*P* adj <0.05) with 1,010 having a fold change of >|1.5| and a *P* adj <0.05 with most of them (922; 91%) being more open in the absence of NR4A3. The more opened DARs in *Nr4a3*$^{-/-}$ cells were enriched for regions containing consensus binding sites for the bZIP family of transcription factors (AP-1, Jun, Fos, and BATF) while the less opened DARs were enriched for NR4A3 and its family members consensus site (NBRE; identified as Nur77 in

the figure) and Fli1 (Fig. 5*B*). Among the DARs (with a cutoff of *P* adj <0.05), 105 of them contained NBRE motifs (Dataset S3) and 25% of them show differential transcription by *Nr4a3*$^{-/-}$ OT-I day-3 effectors (Fig. 5*C*). Among all of the DARs (*P* adj <0.05) at 12 h poststimulation of *Nr4a3*$^{+/+}$ and *Nr4a3*$^{-/-}$ OT-I T cells, 20% of the genes associated with them are differentially transcribed by day-3 in vivo effectors (*P* adj <0.05; *SI Appendix*, Fig. S4*C*). This demonstrates that NR4A3 has an early influence on the transcriptional program of CD8$^+$ T cells with a major impact on genes that are regulated by bZIP transcription factors, which share a similar consensus binding sequence on DNA. The enhanced opening of chromatin regions containing bZIP consensus binding sites is in line with recent reports suggesting that NR4A family members affect the binding of Jun to target genes (33, 35).

Analysis of our RNA-seq data using the GeneXplain platform (40) identifies Fos and Jun as the top upstream master regulators of the differentially expressed genes (Fig. 5*D*) further supporting a role for NR4A3 in modulating the action of the AP-1 transcription factor. Altogether this indicates that the absence of NR4A3 favors the binding of AP-1 and/or other bZIP transcription factors to chromatin to promote the transcription of target genes. Interestingly, AP-1 and Jun are known to promote the transcription of effector genes (14, 41), thus providing a possible explanation for the enhanced effector functions of *Nr4a3*$^{-/-}$ CD8$^+$ T cells.

Discussion

Our results identify that NR4A3 restrains memory potential and effector functions of CD8$^+$ T cells in acute infection. In this context, NR4A3-deficient CD8$^+$ T cells generate more MPECs
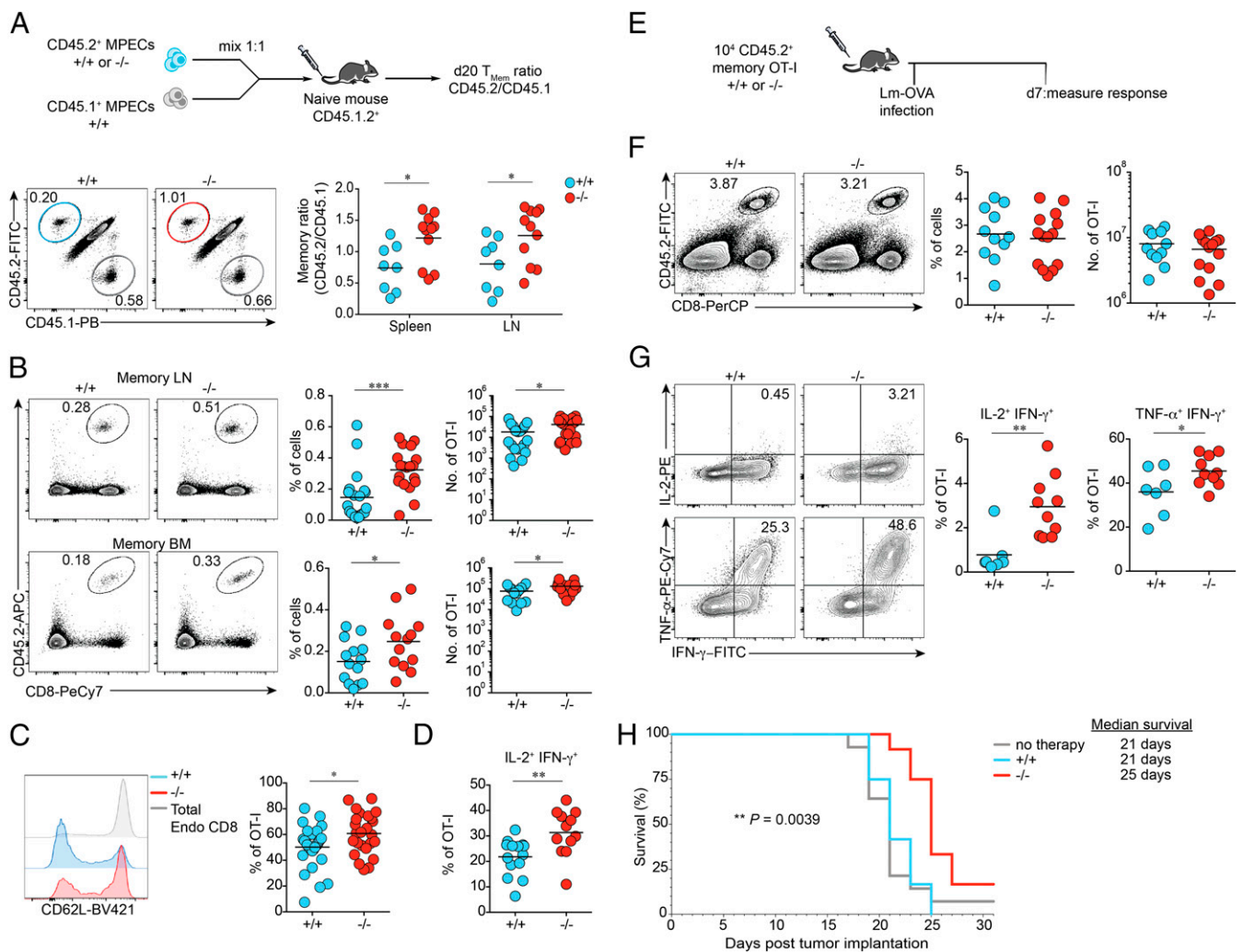
Fig. 3. NR4A3 deficiency promotes MPEC differentiation into memory cells and increases central memory T cell generation. (*A, Top*) Experimental design assessing the potential of *Nr4a3*^{+/+} and *Nr4a3*^{−/−} OT-I MPECs for the formation of memory cells. (*A, Bottom*) The percentage of adoptively transferred CD45.2^{+} memory cells, either [+/+] or [−/−], from spleen and LNs 20 d posttransfer, was normalized to the percentage of CD45.1^{+} cells in order to obtain a ratio of memory generation (representative flow plots are from spleen). (*B*) Memory responses in the LN and bone marrow (BM) of mice adoptively transferred with CD45.2[+] *Nr4a3*^{+/+} or *Nr4a3*^{−/−} OT-I cells prior to Lm-OVA infection. CD62L expression (*C*) and proportion of IL-2 and IFN-γ coproducing (*D*) OT-I memory *Nr4a3*^{+/+} or *Nr4a3*^{−/−} cells in the spleen. (*E*) Experimental design to test the secondary response of *Nr4a3*^{+/+} or *Nr4a3*^{−/−} memory cells. Quantification in the spleen of the response (*F*) and cytokine production (*G*) of secondary effectors *Nr4a3*^{+/+} or *Nr4a3*^{−/−}. (*H*) *Nr4a3*^{+/+} and *Nr4a3*^{−/−} OT-I memory cells were generated in response to Lm-OVA infection. At least 40 d postinfection, ∼2 × 10^{5} *Nr4a3*^{+/+} or *Nr4a3*^{−/−} OT-I memory cells were adoptively transferred into B16-OVA bearing mice (7 d postimplantation). Mouse survival and tumor growth were monitored every 2 d. Each dot represents one mouse. Endo: total endogenous CD8^{+}CD45.2^{−} cells. Survival curves were compared using log-rank Mantel–Cox test (*H*). Data are from two (*A*, [+/+]/CD45.1^{+} competitive group and *H*), or at least three independent experiments. Unpaired Student's *t* test, with a Welch's correction when applied, was used: *$P < 0.05$, **$P < 0.01$, ***$P < 0.001$.

and central memory CD8^{+} T cells while having enhanced capacity to produce cytokines.

At the molecular level, our results demonstrate that NR4A3 influences CD8^{+} T cell differentiation by affecting the chromatin accessibility of certain genes early following CD8^{+} T cell activation, which then leads to a transcriptional program that favors SLEC generation while repressing effector functions. In the absence of NR4A3, most of the DARs are more open and these are significantly enriched for the bZIP (Jun, Fos, AP-1, etc.) family transcription factor motif. This is similar to what has been recently reported for NR4A1 in CD4^{+} T cells and for NR4A triple-deficient CD8^{+} tumor-infiltrating lymphocytes (TILs) (33, 35). Interestingly, NR4A1-deficient CD4^{+} T cells and NR4A triple-deficient CD8^{+} TILs are also more functional than their WT counterpart. This suggests that all three NR4A family members have the ability to influence effector functions and that

they do so using a similar molecular mechanism. It is therefore intriguing that loss of only one member is sufficient to affect T cell functionality. Further studies should reveal whether each member affects a different set of genes controlling T cell functions and that these are possibly regulated by different bZIP transcription factors.

Our molecular analysis also reveals that NR4A3 affects MPEC/SLEC differentiation by controlling the early induction of the SLEC molecular program. It could be considered surprising that NR4A3 restrains both effector functions and memory generation. There are several members of the bZIP transcription factor family and their individual expression varies at different stages of the immune response (17). In the course of an immune response, bZIP transcription factor binding motif is enriched in open chromatin regions of SLECs, MPECs, and memory CD8^{+} T cells when compared to naive cells (17–19). Also, members of
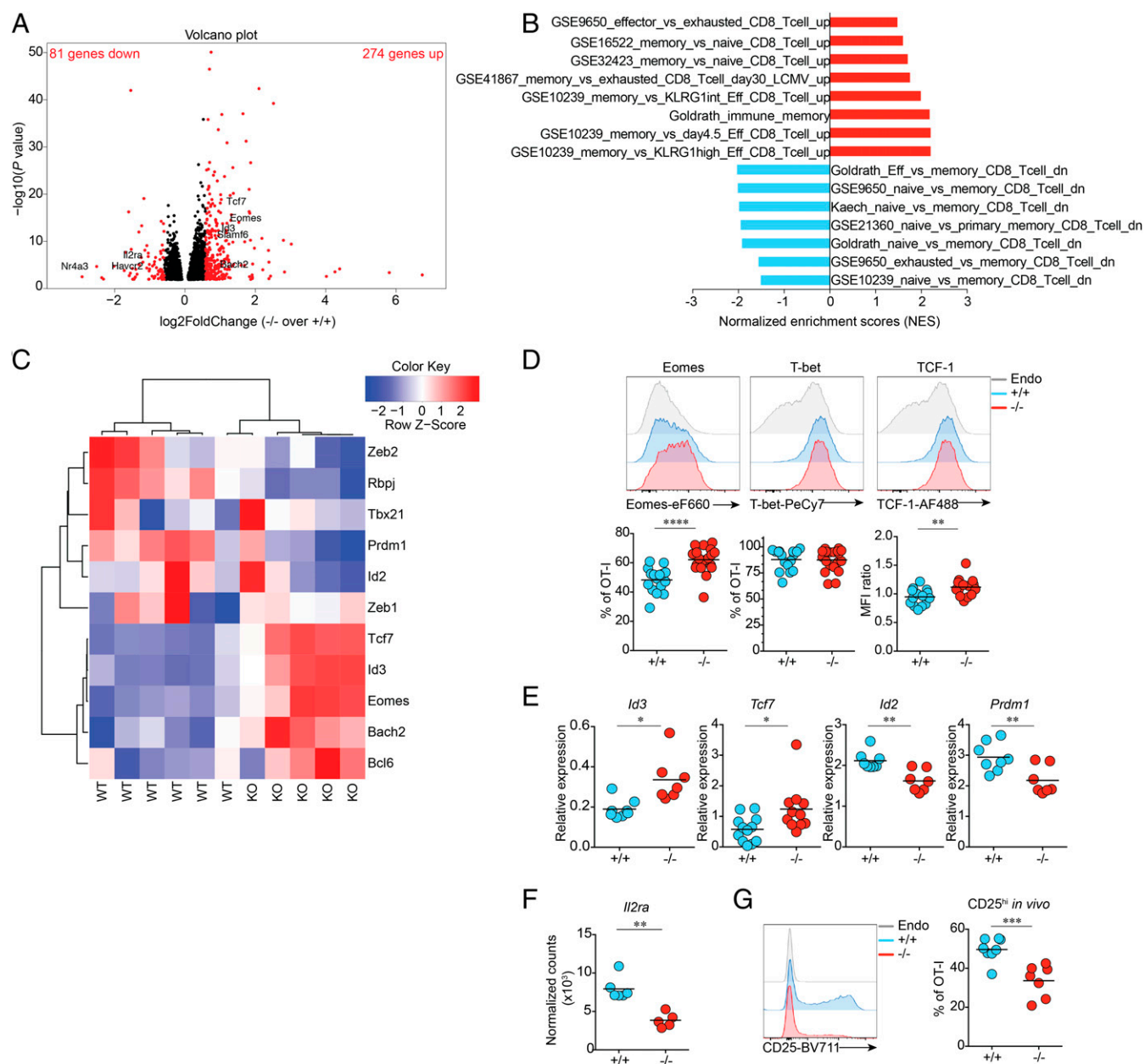
Fig. 4. NR4A3 is an early regulator of the CD8+ T cell memory gene signature. (*A*) Volcano plot of genes differentially expressed in *Nr4a3*^+/+ and *Nr4a3*^−/− OT-I cells assessed by RNA-seq at day 3 postinfection with Lm-OVA. Indicated in black, genes *P* adj <0.05. Indicated in red, genes *P* adj <0.05 and |FC|>1.5. (*B*) GSEA of the NR4A3-regulated transcriptome reveals enrichment of memory signatures. (*C*) Heat map illustrating the relative expression in *Nr4a3*^+/+ and *Nr4a3*^−/− OT-I cells of genes encoding for selected transcription factors controlling CD8+ T cell differentiation. At day 7 post-Lm-OVA infection, the expression of transcription factors known to be involved in CD8+ T cell memory generation was measured by FACS (*D*) or by qRT-PCR (*E*) in spleens. (*F*) *Il2ra* transcription by day-3 OT-I effectors (data from RNA-seq). (*G*) At day 3 post-Lm-OVA infection, expression of CD25 on *Nr4a3*^+/+ and *Nr4a3*^−/− OT-I cells was measured by flow cytometry. Endo: total CD8+CD45.2− endogenous cells. Each dot represents one mouse. Data are from two (*A*, *C*, *E*, and *G*) or at least three independent experiments (*D*). A Mann–Whitney unpaired *t* test (*F*), when a low number of experimental samples were available, was used and an unpaired Student's *t* test, with a Welch's correction when applied, was used for the other two-group comparison: *P < 0.05, **P < 0.01, ***P < 0.001, ****P < 0.0001.

this family have been shown to target promemory genes, such as *Bcl6*, *Tcf7*, and *Eomes*, as well as genes more traditionally associated with effector functions (41). Finally, it is possible that some bZIPs contribute to the acquisition of effector function while others promote memory generation. As a whole, these elements underline the complexity of this family of transcription factors and suggest that, while perhaps counterintuitive at face value, the fact that we observed an enrichment for bZIP motifs in opened chromatin regions of *Nr4a3*^−/− CD8+ T cells early in the response is compatible with both an increase in effector function

and in memory potential. This interpretation is supported by a recent report demonstrating that CAR T cells overexpressing c-Jun are more functional and undergo less terminal differentiation (42).

Intriguingly, NR4A1, which does compete with c-Jun, was reported to have either no effect on MPEC/SLEC differentiation or to limit SLEC formation, which would be the opposite effect of NR4A3 (35, 43). These observations strengthen the notion that the different NR4A family members have nonoverlapping functions during the CD8+ T cell response. While NR4A3 could have a dominant effect over NR4A1 in affecting the binding of
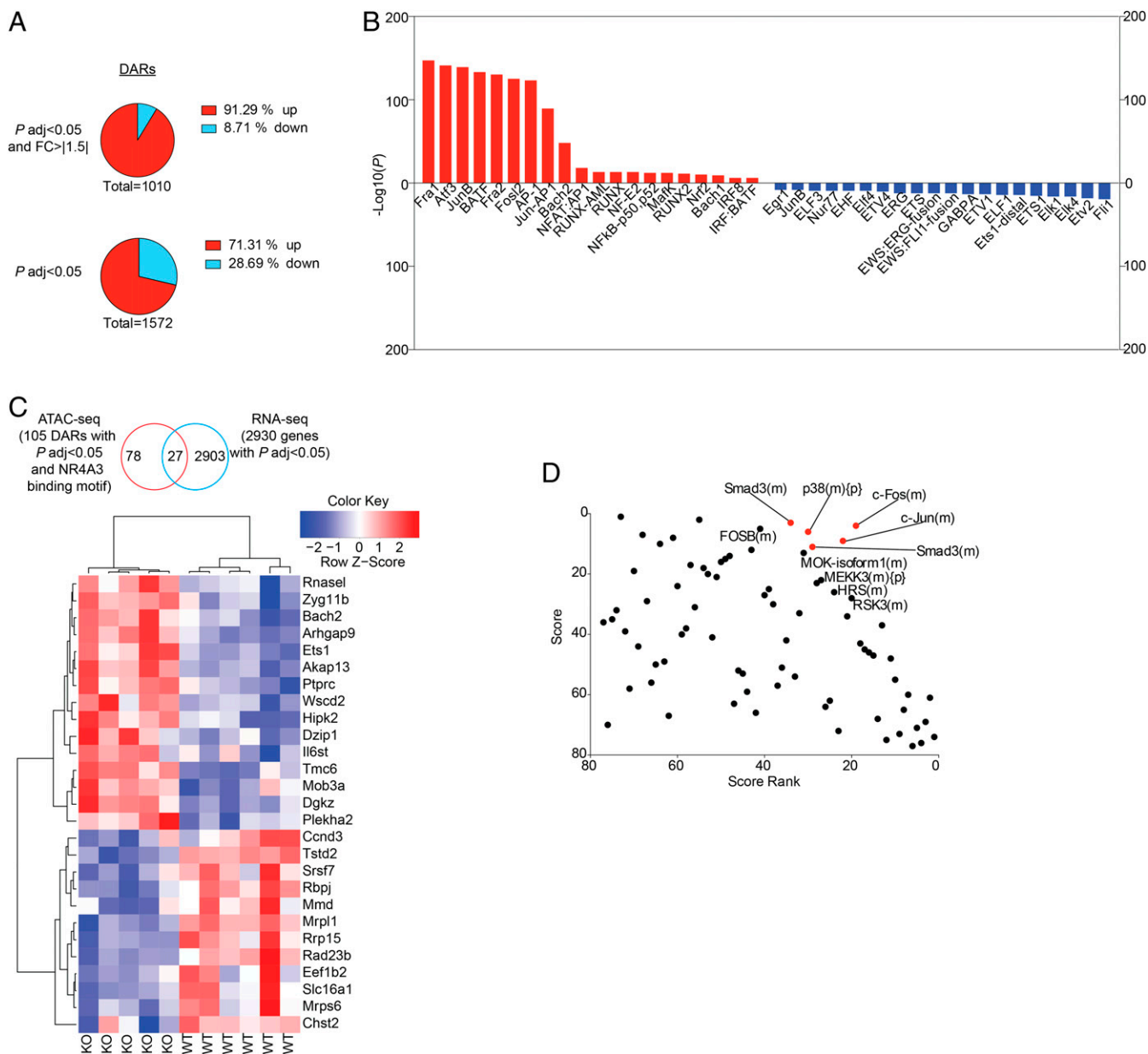
Fig. 5. Early NR4A3 modulation of chromatin accessibility during T cell activation. (*A*) Number of DARs in the chromatin of *Nr4a3*⁻/⁻ versus *Nr4a3*⁺/⁺ OT-I T cells stimulated for 12 h with anti-CD3/CD28 assessed by ATAC-seq (*Top* chart: cutoff of *P* adj <0.05 and |FC|>1.5; *Bottom* chart: cutoff *P* adj <0.05 only). "Up" indicates the proportion of DARs that are more open in *Nr4a3*⁻/⁻ T cells while "down" indicates the proportion of DARs less open in *Nr4a3*⁻/⁻ T cells, compared to *Nr4a3*⁺/⁺ T cells. (*B*) Transcription factor motif enrichment analysis of DARs that are more open in *Nr4a3*⁻/⁻ cells (red bars) or less open in *Nr4a3*⁻/⁻ cells (blue bars). (*C*) Analysis of the genes found to be regulated by *Nr4a3* at day 3 postinfection by RNA-seq analysis and linked to NR4A motif containing DARs between *Nr4a3*⁺/⁺ and *Nr4a3*⁻/⁻ T cells determined by ATAC-seq. (*D*) RNA-seq data comparing *Nr4a3*⁺/⁺ and *Nr4a3*⁻/⁻ T cells expression profiles were submitted to upstream master regulator analysis in the GeneXplain platform. Top-ranked upstream regulators have the lowest rank sum value, obtained by adding the score and score rank. The top five results are highlighted in red. ATAC-seq experiment was performed once on two biological samples of each genotype.

bZIP transcription factors to their target genes or could selectively affect the binding of certain bZIP transcription factor family members, it is also possible that the increased MPEC formation in *Nr4a3*⁻/⁻ mice was not solely the consequence of enhanced accessibility of bZIP transcription factors to DNA. NR4A3's transcriptional effects could be mediated by a direct regulation of NR4A3 via binding on genes containing an NBRE motif in conjunction with the reported ability of NR4As to modulate chromatin remodeling (44). Among the differentially accessible chromatin regions between *Nr4a3*⁺/⁺ and *Nr4a3*⁻/⁻

activated OT-I T cells, 105 of them contain a putative NBRE motif (Dataset S3). Very few of these regions are in proximity of genes known to influence SLEC/MPEC differentiation and effector functions. These include *Rbpj* and *Bach2* (8, 9, 14). While we found DARs in proximity to genes related to CD8⁺ T cell differentiation or function, such as *Il2ra*, *Irf4*, and *Myc*, these regions did not contain classical NBRE motifs (37, 45–48). In other studies looking at early in vitro T cell activation or in TILs, NBRE motifs were found close to *Foxo1*, *Havcr2*, *Kit*, *Tcf7*, *Tbx21*, *Id3*, and *Bcl6*, but we did not detect a difference in

chromatin opening at these sites in our study (19, 33). Because the expression of some of these genes was differential in our RNA-seq, NR4A3 could regulate their expression, but not by influencing the accessibility of chromatin. Alternatively, we might have missed these important sites because we elected to perform our ATAC-seq study at 12 h poststimulation. This decision was motivated by the desire to uncover the early events mediated by NR4A3 whose peak of TCR-induced mRNA expression was identified at 12 h. However, NR4A3 protein expression could be maintained for a longer period of time and there could be NR4A3-regulated targets of importance at later time points. Another possibility is the reported ability of NR4A family members to regulate transcription without directly binding to DNA. This process of transrepression was shown in myeloid cells and is the result of interaction of NR4A2 with the p65 subunit of NFκB, which favors the recruitment of CoREST that actively removes p65 from the promoters of inflammatory genes (49). Relevant to this, note that NFκB binding motif is also enriched in our ATAC-seq data. Overall, this highlights the complexity of the NR4A family and underlies the need for further mechanistic studies.

The NR4A family members are induced by TCR signaling, and may thus be important during thymic T cell differentiation or play a role in the maintenance of memory cells following tonic signaling. Lack of NR4A3 expression during thymic differentiation could impact the response of peripheral mature CD8+ T cells. We think that this is an unlikely possibility as overexpression of NR4A3 after activation of naive $Nr4a3^{-/-}$ CD8+ T cells was able to recapitulate the WT phenotype for MPEC/SLEC differentiation and cytokine production. In support of this, thymic differentiation and peripheral T cell phenotype was not affected by NR4A3 deficiency. We have also not formally excluded a role for NR4A3 in regulating CD8+ T cell memory in response to tonic signaling. However, as expected for an immediate early gene, during an acute response $Nr4a3$ transcription is already abolished at day 2 in vivo (*SI Appendix*, Fig. S5 and ref. 20). In addition, data suggest that in both T cells and B cells, NR4A3 is not induced following tonic signaling, contrary to what was observed for NR4A1 (50, 51). This, coupled to our sequencing data obtained early following TCR stimulation support that the impact of NR4A3 on CD8+ T cell differentiation is not likely to be via a role in the response of memory T cells to tonic signaling. It would be of interest to confirm this using an inducible cre/lox system. However, growing evidence demonstrates that in tertiary tissue, NR4A family members are reexpressed and important for resident memory T cells, suggesting that the biological role of NR4As could be dependent on tissue microenvironment (52–55).

Altogether, our results suggest that the modulation of NR4A3 activity represents a promising avenue for enhancing the generation of memory CD8+ T cell following vaccination and for the production of better T cells for adoptive cell therapy of cancer patients.

Materials and Methods

Mice. B6.SJL, C57BL/6, CD45.1.2 (F1 of B6.SJL × C57BL/6), $Nr4a3^{-/-}$ and $Nr4a3^{+/+}$, OT-I (36) ($Rag1^{-/-}$ CD45.2) mice were all bred at the Maisonneuve-Rosemont Hospital Research Center facility. $Nr4a3^{-/-}$ mice were a kind gift from Orla M. Conneely (Baylor College of Medicine, Houston, TX; 56). OT-I/B6.SJL mice were obtained by crossing OT-I ($Rag1^{-/-}$ CD45.2) mouse with B6.SJL (CD45.1). $Nr4a3^{-/-}$ were backcrossed for at least 10 generations to C57BL/6 and then crossed to OT-I mouse to obtain OT-I $Nr4a3^{+/+}$ ($Rag1^{-/-}$ CD45.2) and OT-I $Nr4a3^{-/-}$ ($Rag1^{-/-}$ CD45.2) mice. Mice were housed in a pathogen-free environment and treated in accordance with the Canadian Council on Animal Care guidelines.

Cell Lines. B16-OVA cells were kindly provided by A. Lamarre, Institut National de la Recherche Scientifique-Institut Armand-Frappier, Laval, QC, Canada. B16-OVA cells were cultured in Dulbecco's Modified Eagle Medium (DMEM) supplemented with 10% of *Nu* serum, sodium pyruvate (1 mM), penicillin/streptomycin in presence of 5 mg/mL G418 to select for OVA expressing cells. HEK293T cells were kindly provided by H. Melichar, University of Montreal, Montreal, QC, Canada and cultured in DMEM supplemented with 10% of *Nu* serum and penicillin/streptomycin.

Adoptive Transfer and Immune Responses. For the study of effector and memory CD8+ T cell generation, 5×10^3 to 10^4 $Nr4a3^{+/+}$ or $Nr4a3^{-/-}$ OT-I CD8+ T cells (CD45.2+) isolated from lymph nodes (LNs) were adoptively transferred into recipients by i.v. injection. The following day, mice were infected or vaccinated as described below. For the study of the early in vivo immune response (days 1 to 3), 2×10^6 OT-I T cells were adoptively transferred. For competitive experiments, 10^4 $Nr4a3^{+/+}$ or $Nr4a3^{-/-}$ OT-I T cells (CD45.2+) were cotransferred with 10^4 WT B6.SJL OT-I T cells (CD45.1+) into CD45.1.2 recipients.

Lm-OVA Infection. A total of 2×10^3 CFU of *L. monocytogenes* genetically modified to express OVA (Lm-OVA) [grown as previously described (57, 58)] was injected i.v. For analysis of secondary response, 10^4 $Nr4a3^{+/+}$ or $Nr4a3^{-/-}$ (CD45.2+), generated in vivo following Lm-OVA infection, were adoptively transferred into a B6.SJL (CD45.1+). On the following day, mice were infected with 10^4 CFUs of Lm-OVA. The secondary response was evaluated at day 7 postinfection.

LCMV-OVA Infection. The strain of LCMV Armstrong encoding OVA (LCMV-OVA) was kindly provided by Juan C. de la Torre, The Scripps Research Institute, La Jolla, CA (59). The virus was produced by infection of the L929 fibroblast cell line, cultured in Minimum Essential Medium (MEM) containing 5% heat inactivated *Nu* serum, followed by harvesting of the produced virus in the supernatant. The virus titer was determined using MC57G fibroblasts as previously described (60). Mice were infected with 2×10^4 PFUs of LCMV-OVA by i.v. injection.

Dendritic Cell Immunization. Dendritic cell (DC) immunization was performed as previously described (38). Bone marrow cells were cultured at 0.25×10^6 cells/mL in six-well plates in complete media supplemented with recombinant granulocyte-macrophage colony-stimulating factor (rGM-CSF; 25 ng/mL) and IL-4 (from P815-IL-4 cell culture supernatant). On days 2 and 3 of the differentiation culture, half of the media was removed and replaced with a fresh IL-4 and rGM-CSF supplemented complete media. On day 6, lipopolysaccharides (LPS; 0.1 μg/mL) was added to mature DCs and OVA peptide was loaded overnight (2 μg/mL). For immunization, 5×10^5 OVA peptide loaded DCs were injected i.v.

Analysis of Polyclonal CD8+ T Cell Response following Lm-OVA Infection. At day 7 postinfection with Lm-OVA (2×10^3 CFUs, i.v.), the response of OVA-specific CD8+ T cells in the spleen was evaluated using K^b-OVA tetramer staining as previously described (9).

Retroviral Supernatant Production. pMSCV IRES GFP (plasmid of murine stem cell virus with internal ribosome entry site element with GFP also called pMIG) was a kind gift from Guy Sauvageau (Institut de recherche en immunologie et en cancérologie IRIC, Montreal, QC, Canada, 61) and pMIG-$Nr4a3$ has been previously described (23). Retroviral supernatants were produced by collecting the cell culture media at days 2 and 3 after transfection of HEK293T cells with pMIG or pMIG-$Nr4a3$.

$Nr4a3$ Retroviral Overexpression. $Nr4a3^{+/+}$ or $Nr4a3^{-/-}$ OT-I T cells (CD45.2+) were isolated from LNs and mixed with B6.SJL spleen (CD45.1+) cells in a 2:3 ratio. Cells were cultured at 5×10^6 cells/mL in the presence of 0.1 μg/mL of OVA peptide. At 24 h poststimulation, cells were harvested and spin transduced with retroviral supernatant (pMIG retrovirus [RV] or pMIG $Nr4a3$ containing RV) in the presence of polybrene (8 μg/mL) for 1 h at 2,500 rpm and 37 °C. The cells were incubated for an additional 1 to 2 h at 37 °C and then injected (3×10^5 OT-I cells) in mice infected 24 h earlier with Lm-OVA (2×10^3 CFU/mouse).

MPEC Competitive Transfer. A total of 10^6 $Nr4a3^{+/+}$ or $Nr4a3^{-/-}$ OT-I T cells (CD45.2+) were adoptively transferred in competition with 10^6 OT-I T cells (CD45.1+) from B6.SJL mice into CD45.1+CD45.2+ mice. The following day, recipient mice were infected with 2×10^3 CFUs of Lm-OVA. At day 5 postinfection, spleens were harvested to sort $Nr4a3^{+/+}$ or $Nr4a3^{-/-}$ OT-I MPECs (CD8+CD45.2+CD127+KLRG1−) and WT OT-I MPECs (CD8+CD45.1+ CD127+ KLRG1−). A total of 1 to 2×10^5 MPECs of each genotype were mixed in a

1:1 ratio and transferred into CD45.1+CD45.2+ recipient mice. Twenty days later, spleens and LNs were harvested to track OT-I T cell differentiation.

Stimulation of Memory T Cells with rhIL-15. Splenocytes (10^6/mL) from mice containing OT-I memory T cells were labeled with CellTrace Violet (CTV) and cultured with 50 ng/mL of rhIL-15 (R&D) for 3 d.

Adoptive Cell Therapy with In Vivo Generated Memory T Cells. B6.SJL mice were injected s.c. with 5×10^5 B16-OVA cells into the right flank. Seven days posttumor implantation, tumor-bearing mice were treated with $1.35-2 \times 10^5$ in vivo generated *Nr4a3*+/+ or *Nr4a3*−/− OT-I memory T cells obtained following Lm-OVA infection. Tumor growth was followed until experimental endpoint (200 mm² or tumor ulceration) was reached.

Samples Preparation for Flow Cytometry Analysis. Blood was collected in phosphate buffered saline (PBS) containing 2 mM ethylenediaminetetraacetic acid (EDTA) and lymphocytes were isolated with lymphocyte separation medium. Spleens and LNs were dissociated using frosted glass slides. Red blood cell lysis was performed on spleens and bone marrow using 0.83% NH₄Cl for 5 min at room temperature (RT). Extracellular staining was performed for 20 min at 4 °C as in a previously described FACS wash (FW) buffer (62). Intranuclear staining for different transcription factors was performed using the Foxp3/Transcription Factor Staining Buffer Set according to manufacturer (Invitrogen) instructions.

Lm-OVA Challenge. Mice that were previously adoptively transferred with OT-I T cells and infected with LCMV-OVA (as described above) were challenged at day 43 with 5×10^5 CFUs of Lm-OVA. On day 3 postchallenge, spleen and liver were collected for analysis of bacterial burdens as previously described (57).

Flow Cytometry and Cell Sorting. Flow cytometry was performed on cellular suspensions of spleen, LN, bone marrow, and blood. Extracellular and intranuclear stainings were performed as previously described (57, 62, 63). CTV staining was performed according to the manufacturer (Thermo Fisher) recommendations. Apoptosis was quantified using AnnexinV and 7-amino-actinomycin D (7-AAD) staining as previously described (38). Ki67 staining was performed by using FoxP3 Transcription Factor Staining Kit following manufacturer recommendations. At 2 wk following bromodeoxyuridine (BrdU) treatment (64), BrdU staining was performed as previously described (38). Cell sorting of OT-I *Nr4a3*+/+ or *Nr4a3*−/− cells was performed on in vitro stimulated or ex vivo splenocytes. Briefly, cell suspensions were incubated with viability dye and Fc-block antibodies for 10 min at RT. Cell suspensions were then stained with extracellular antibodies 20 min at 4 °C in sorting buffer (PBS, 1% *Nu* serum, 1 mM EDTA, 25 mM Hepes). Viable cells (Zombie-dye^neg CD8+CD45.2+) were then sorted (BD FACSAria III) directly in TRIzol (Life Technologies) reagent and stored at −80 °C until RNA extraction or sorted in serum-containing media (20% *Nu* serum containing RPMI) for subsequent use. For cytokine production by retrovirally transduced OT-I T cells, CD8+CD45.2+GFP+ or CD8+CD45.2+GFP− cells were sorted and then restimulated as described below. Flow cytometry analysis was performed on a BD LSR II or BD LSRFortessa X-20 from BD Biosciences and data were analyzed using FlowJo software (Tree Star). A list of antibodies and flow cytometry reagents is provided in *SI Appendix*, Table S1.

Analysis of Cytokine Production. Ex vivo splenocytes were collected and stimulated with the OVA peptide (2 µg/mL) in the presence of brefeldin A (BFA, 10 µg/mL) for 5 h at 37 °C while in vitro activated OT-I effectors were restimulated with OVA-loaded splenocytes. Following stimulation, cells were fixed, permeabilized, and stained as previously described (63). Briefly, restimulated cells were fixed 20 min with 2% paraformaldehyde at RT. Fixed cells were permeabilized with saponin (0.5%) FW for 10 min at RT. Permeabilized cells were stained with anti-cytokine antibodies followed by cell surface staining.

Anti-CD3/CD28 Stimulation. A total of 10^6 cells/mL from LNs of OT-I mice were stimulated in 24-well plates with 1 µg of plate-bound anti-CD3 (clone 145-2C11) antibody and 5 µg/mL soluble anti-CD28 (clone 37.51) antibody for 72 h.

Quantitative Real-Time PCR. Total RNA from cells sorted in TRIzol was extracted using manufacturer recommendations. RNA was reverse-transcribed into cDNA and then used for the qPCR reaction with Power SYBR Green reagents (Life Technologies) on a 7500 Real-Time PCR System (Applied Biosystems).

Each sample was normalized to a reference gene expression (*Hprt*) and a calibrator (reference sample) as previously described (57). ΔC_T was calculated as the difference between the C_T value of the target gene and the C_T value of the reference gene (*Hprt*). The $\Delta\Delta C_T$ was then calculated by subtracting the mean of ΔC_T value of the sample from the ΔC_T value of a reference sample. The relative level of target gene expression was calculated using $2^{-\Delta\Delta C_T}$. The sequences of the *Id2*, *Id3*, *Tcf7*, *Prdm1*, *Il2*, *Tnfa*, and *Ifng* primers are listed in *SI Appendix*, Table S1.

RNA-Seq Analysis. Mice were adoptively transferred with naive OT-I T cells purified with the EasySep Isolation Kit and infected with Lm-OVA. At 72 h postinfection, viable and activated (Zombie-dye^neg CD44^hi) *Nr4a3*+/+ or *Nr4a3*−/− OT-I T cells were sorted directly into TRIzol reagent. A total of 5 to 6 individual biological samples (2 to 3 mice per group of two independent experiments) were collected for each genotype with 10^5 cells per sample. RNA extraction, library preparation, sequencing, and bioinformatical analysis were done at the IRIC Genomics Platform (University of Montreal). Briefly, for cDNA libraries preparation, 100 ng of RNA was used and the cDNA library sequencing was performed on Illumina Nextseq500 (75 cycles single-end reads). Sequenced reads were trimmed for sequencing adapters and low-quality 3′ bases using Trimmomatic version 0.35 (65) and then aligned to the reference mouse genome version GRCh38 (gene annotation from Gencode version M13, based on Ensembl 88) using STAR version 2.5.1b (66). Gene expressions were obtained both as readcount directly from STAR as well as computed using RSEM (67) in order to obtain gene and transcript-level expression, either in transcripts per kilobase million or fragments per kilo base per million mapped reads values, for these stranded RNA libraries. DESeq2 version 1.22.2 (68) was then used to normalize gene readcounts and compute differential expression between the different experimental conditions.

ATAC-Seq Analysis. *Nr4a3*+/+ or *Nr4a3*−/− OT-I T cells were isolated from LNs and purified using the naive CD8+ T cell isolation kit of EasySep according to the manufacturer instructions. Isolated naive OT-I T cells were stimulated as described in *Materials and Methods* with anti-CD3/CD28 antibodies. At 12 h poststimulation, cells were harvested and nuclei isolated as previously described (69). Briefly, the stimulated OT-I cells were harvested on ice by washing the stimulation plates with ice-cold PBS. The collected cells were centrifuged 5 min at 1,300 rpm and then resuspended to 20×10^6 cells per mL with ice-cold PBS. The cell lysis was performed for 10 min on ice by adding to one volume of ice-cold PBS resuspended cells four volumes of lysis buffer (12.5 mM Tris, pH 7.4, 45 mM KCl, 6.25 mM MgCl₂, 375 mM sucrose, 0.125% Nonidet P-40, and tablet of complete [EDTA free] protease inhibitor mixture [Roche]/50 mL). Lysed cells were then centrifuged at $500 \times g$ for 7 min at 4 °C in a precooled centrifuge with swinging buckets. Obtained nuclei pellet was resuspended by pipetting in 1/10 of the original lysis volume in wash buffer (10 mM Tris, pH 7.4, 60 mM KCl, 15 mM NaCl, 5 mM MgCl₂, 300 mM sucrose) and then the wash buffer was added to 1/2 of the lysis volume. The resuspended nuclei were centrifuged at $500 \times g$ 7 min at 4 °C in a precooled centrifuge with swinging buckets and the washed nuclei were counted and used for the transposase reaction. ATAC-seq was performed as previously described (70) with some modifications (Tn5 tagmentation, DNA purification, library preparation, and sequencing and bioinformatical analysis were performed at the Montreal Clinical Research Institute Genomics Platform at the University of Montreal). Briefly, 5×10^4 nuclei were directly treated with *Tn5* transposase at 37 °C for 30 min. After the enzymatic reaction, the DNA was purified by Mini-Elute PCR Purification columns (Qiagen) and enriched by 12 cycles of PCR. The library was recovered from PCR by GeneRead Purification columns (Qiagen) and then it was double-strand sequenced on Illumina (HiSeq4000 PE50). A total of 47.3 to 75 × 10^6 reads/sample were obtained. These reads were assessed for quality control with FASTQC (0.11.8) and combined with MultiQC. The adapters were removed with Trimmomatic (0.36) (71) and reads were aligned with Bowtie2 (2.2.6) (72) to *mm10* mouse genome. Mitochondrial reads and PCR duplicates were removed with Picard's MarkDuplicates tools (2.4.1) and shift reads of Tn5 insertion were determined with Deeptools (73). Peaks calling was done with MACS2 (2.0.10) (74) and their filtering with ENCODE black-listed regions. Comparison of DARs between 12-h stimulated OT-I *Nr4a3*−/− and *Nr4a3*+/+ samples was performed with DESeq2 (1.22.2) (75). The log2FC was calculated between *Nr4a3*−/− and *Nr4a3*+/+ conditions; a positive DAR value means that the chromatin is more open in the *Nr4a3*−/− sample and a negative DAR value means that the chromatin is more open in the *Nr4a3*+/+ sample. DARs were annotated and different transcription binding motifs identified with HOMER (4.8.0). Tn5 tagmentation, DNA purification, library preparation, and sequencing and bioinformatical analysis were performed

at the Montreal Clinical Research Institute (IRCM) Genomics Platform (University of Montreal).

Statistical Analyses. Statistical analyses were performed using an unpaired (two tailed) Student's t test, with a Welch's correction when applied, or using a Mann–Whitney test when a low number of samples (lower than seven samples) was available. For multiple group comparisons, the one-way ANOVA (Kruskal–Wallis) analysis with Dunn's multiple comparisons was performed. For survival curve comparison a log-rank Mantel–Cox test was used. The statistical analysis was performed using Prism software (GraphPad Software). Data are presented as individual samples with mean and $*P < 0.05$, $**P < 0.01$, $***P < 0.001$, $****P < 0.0001$ were considered statistically significant.

Data and Materials Availability. The raw RNA-seq and ATAC-seq data are available in the Gene Expression Omnibus (GSE143513) (76) and the analyzed results are presented in the supplemental materials. All other data needed to evaluate the conclusions of this paper are presented in the figures or the supplementary materials.

1. S. M. Kaech et al., Selective expression of the interleukin 7 receptor identifies effector CD8 T cells that give rise to long-lived memory cells. *Nat. Immunol.* **4**, 1191–1198 (2003).
2. N. S. Joshi et al., Inflammation directs memory precursor and short-lived effector CD8(+) T cell fates via the graded expression of T-bet transcription factor. *Immunity* **27**, 281–295 (2007).
3. S. Sarkar et al., Functional and genomic profiling of effector CD8 T cell subsets with distinct memory fates. *J. Exp. Med.* **205**, 625–640 (2008).
4. R. L. Rutishauser et al., Transcriptional repressor Blimp-1 promotes CD8(+) T cell terminal differentiation and represses the acquisition of central memory T cell properties. *Immunity* **31**, 296–308 (2009).
5. A. Kallies, A. Xin, G. T. Belz, S. L. Nutt, Blimp-1 transcription factor is required for the differentiation of effector CD8(+) T cells and memory responses. *Immunity* **31**, 283–295 (2009).
6. C. Y. Yang et al., The transcriptional regulators Id2 and Id3 control the formation of distinct memory CD8+ T cell subsets. *Nat. Immunol.* **12**, 1221–1229 (2011).
7. Y. Ji et al., Repression of the DNA-binding inhibitor Id3 by Blimp-1 limits the formation of memory CD8+ T cells. *Nat. Immunol.* **12**, 1230–1237 (2011).
8. R. A. Backer et al., A central role for Notch in effector CD8(+) T cell differentiation. *Nat. Immunol.* **15**, 1143–1151 (2014).
9. M. Mathieu, F. Duval, J. F. Daudelin, N. Labrecque, The Notch signaling pathway controls short-lived effector CD8+ T cell differentiation but is dispensable for memory generation. *J. Immunol.* **194**, 5654–5662 (2015).
10. K. D. Omilusik et al., Transcriptional repressor ZEB2 promotes terminal differentiation of CD8+ effector and memory T cell populations during infection. *J. Exp. Med.* **212**, 2027–2039 (2015).
11. C. X. Dominguez et al., The transcription factors ZEB2 and T-bet cooperate to program cytotoxic T cell terminal differentiation in response to LCMV viral infection. *J. Exp. Med.* **212**, 2041–2056 (2015).
12. A. M. Intlekofer et al., Effector and memory CD8+ T cell fate coupled by T-bet and eomesodermin. *Nat. Immunol.* **6**, 1236–1244 (2005).
13. H. Ichii et al., Role for Bcl-6 in the generation and maintenance of memory CD8+ T cells. *Nat. Immunol.* **3**, 558–563 (2002).
14. R. Roychoudhuri et al., BACH2 regulates CD8(+) T cell differentiation by controlling access of AP-1 factors to enhancers. *Nat. Immunol.* **17**, 851–860 (2016).
15. X. Zhou et al., Differentiation and persistence of memory CD8(+) T cells depend on T cell factor 1. *Immunity* **33**, 229–240 (2010).
16. J. T. Chang et al., Asymmetric T lymphocyte division in the initiation of adaptive immune responses. *Science* **315**, 1687–1691 (2007).
17. J. P. Scott-Browne et al., Dynamic changes in chromatin accessibility occur in CD8+ T cells responding to viral infection. *Immunity* **45**, 1327–1340 (2016).
18. B. Yu et al., Epigenetic landscapes reveal transcription factors that regulate CD8+ T cell differentiation. *Nat. Immunol.* **18**, 573–582 (2017).
19. D. Wang et al., The transcription factor Runx3 establishes chromatin accessibility of cis-regulatory landscapes that drive memory cytotoxic T lymphocyte formation. *Immunity* **48**, 659–674.e6 (2018).
20. J. A. Best et al.; Immunological Genome Project Consortium, Transcriptional insights into the CD8(+) T cell response to infection and memory T cell formation. *Nat. Immunol.* **14**, 404–412 (2013).
21. M. A. Pearen, G. E. O. Muscat, Minireview: Nuclear hormone receptor 4A signaling: Implications for metabolic disease. *Mol. Endocrinol.* **24**, 1891–1903 (2010).
22. R. N. Hanna et al., The transcription factor NR4A1 (Nur77) controls bone marrow differentiation and the survival of Ly6C- monocytes. *Nat. Immunol.* **12**, 778–785 (2011).
23. S. Boulet et al., The orphan nuclear receptor NR4A3 controls the differentiation of monocyte-derived dendritic cells following microbial stimulation. *Proc. Natl. Acad. Sci. U.S.A.* **116**, 15150–15159 (2019).
24. S. E. Mullican et al., Abrogation of nuclear receptors Nr4a3 and Nr4a1 leads to development of acute myeloid leukemia. *Nat. Med.* **13**, 730–735 (2007).
25. L. M. Carlin et al., Nr4a1-dependent Ly6C(low) monocytes monitor endothelial cells and orchestrate their disposal. *Cell* **153**, 362–375 (2013).
26. R. N. Hanna et al., NR4A1 (Nur77) deletion polarizes macrophages toward an inflammatory phenotype and increases atherosclerosis. *Circ. Res.* **110**, 416–427 (2012).
27. T. Sekiya et al., Nr4a receptors are essential for thymic regulatory T cell development and immune homeostasis. *Nat. Immunol.* **14**, 230–237 (2013).
28. M. S. Fassett, W. Jiang, A. M. D'Alise, D. Mathis, C. Benoist, Nuclear receptor Nr4a1 modulates both regulatory T-cell (Treg) differentiation and clonal deletion. *Proc. Natl. Acad. Sci. U.S.A.* **109**, 3891–3896 (2012).
29. Q. N. Hu, A. Y. W. Suen, L. M. Henao Caviedes, T. A. Baldwin, Nur77 regulates nondeletional mechanisms of tolerance in T cells. *J. Immunol.* **199**, 3147–3157 (2017).
30. G. P. Mognol et al., Exhaustion-associated regulatory regions in CD8+ tumor-infiltrating T cells. *Proc. Natl. Acad. Sci. U.S.A.* **114**, E2776–E2785 (2017).
31. K. E. Pauken et al., Epigenetic stability of exhausted T cells limits durability of reinvigoration by PD-1 blockade. *Science* **354**, 1160–1165 (2016).
32. G. J. Martinez et al., The transcription factor NFAT promotes exhaustion of activated CD8+ T cells. *Immunity* **42**, 265–278 (2015).
33. J. Chen et al., NR4A transcription factors limit CAR T cell function in solid tumours. *Nature* **567**, 530–534 (2019).
34. H. Seo et al., TOX and TOX2 transcription factors cooperate with NR4A transcription factors to impose CD8+ T cell exhaustion. *Proc. Natl. Acad. Sci. U.S.A.* **116**, 12410–12415 (2019).
35. X. Liu et al., Genome-wide analysis identifies NR4A1 as a key mediator of T cell dysfunction. *Nature* **567**, 525–529 (2019).
36. K. A. Hogquist et al., T cell receptor antagonist peptides induce positive selection. *Cell* **76**, 17–27 (1994).
37. V. Kalia et al., Prolonged interleukin-2Ralpha expression on virus-specific CD8+ cells favors terminal-effector differentiation in vivo. *Immunity* **32**, 91–103 (2010).
38. S. Boulet, J.-F. Daudelin, N. Labrecque, IL-2 induction of Blimp-1 is a key in vivo signal for CD8+ short-lived effector T cell differentiation. *J. Immunol.* **193**, 1847–1854 (2014).
39. J. Arsenio et al., Early specification of CD8+ T lymphocyte fates during adaptive immunity revealed by single-cell gene-expression analyses. *Nat. Immunol.* **15**, 365–372 (2014).
40. E. Wingender, A. Kel, geneXplain–Eine integrierte Bioinformatik-Plattform. *BIOspektrum (Heidelb.)* **18**, 554–556 (2012).
41. M. Kurachi et al., The transcription factor BATF operates as an essential differentiation checkpoint in early effector CD8+ T cells. *Nat. Immunol.* **15**, 373–383 (2014).
42. R. C. Lynn et al., c-Jun overexpression in CAR T cells induces exhaustion resistance. *Nature* **576**, 293–300 (2019).
43. H. N. Nowyhed, T. R. Huynh, G. D. Thomas, A. Blatchley, C. C. Hedrick, Cutting edge: The orphan nuclear receptor Nr4a1 regulates CD8+ T cell expansion and effector function through direct repression of Irf4. *J. Immunol.* **195**, 3515–3519 (2015).
44. R. P. Duren, S. P. Boudreaux, O. M. Conneely, Genome wide mapping of NR4A binding reveals cooperativity with ETS factors to promote epigenetic activation of distal enhancers in acute myeloid leukemia cells. *PLoS One* **11**, e0150450 (2016).
45. K. Man et al., The transcription factor IRF4 is essential for TCR affinity-mediated metabolic programming and clonal expansion of T cells. *Nat. Immunol.* **14**, 1155–1165 (2013).
46. F. Raczkowski et al., The transcription factor Interferon Regulatory Factor 4 is required for the generation of protective effector CD8+ T cells. *Proc. Natl. Acad. Sci. U.S.A.* **110**, 15019–15024 (2013).
47. R. Wang et al., The transcription factor Myc controls metabolic reprogramming upon T lymphocyte activation. *Immunity* **35**, 871–882 (2011).
48. C. Chou et al., c-Myc-induced transcription factor AP4 is required for host protection mediated by CD8+ T cells. *Nat. Immunol.* **15**, 884–893 (2014).
49. K. Saijo et al., A Nurr1/CoREST pathway in microglia and astrocytes protects dopaminergic neurons from inflammation-induced death. *Cell* **137**, 47–59 (2009).
50. A. E. Moran et al., T cell receptor signal strength in Treg and iNKT cell development demonstrated by a novel fluorescent reporter mouse. *J. Exp. Med.* **208**, 1279–1289 (2011).
51. E. Jennings et al., Differential Nr4a1 and Nr4a3 expression discriminates tonic from activated TCR signalling events in vivo. bioRxiv:10.1101/767566v2 (15 January 2020).
52. J. J. Milner et al., Runx3 programs CD8+ T cell residency in non-lymphoid tissues and tumours. *Nature* **552**, 253–257 (2017).
53. L. K. Beura et al., T cells in nonlymphoid tissues give rise to lymph-node-resident memory T cells. *Immunity* **48**, 327–338.e5 (2018).

IMMUNOLOGY AND INFLAMMATION

54. C. S. Boddupalli *et al.*, ABC transporters and NR4A1 identify a quiescent subset of tissue-resident memory T cells. *J. Clin. Invest.* **126**, 3905–3916 (2016).

55. N. S. Kurd *et al.*, Early precursors and molecular determinants of tissue-resident memory CD8+ T lymphocytes revealed by single-cell RNA sequencing. *Sci. Immunol.* **5**, eaaz6894 (2020).

56. T. Ponnio, Q. Burton, F. A. Pereira, D. K. Wu, O. M. Conneely, The nuclear receptor Nor-1 is essential for proliferation of the semicircular canals of the mouse inner ear. *Mol. Cell. Biol.* **22**, 935–945 (2002).

57. M. Mathieu *et al.*, CD40-activated B cells can efficiently prime antigen-specific naïve CD8+ T cells to generate effector but not memory T cells. *PLoS One* **7**, e30139 (2012).

58. K. S. Bahjat *et al.*, Cytosolic entry controls CD8+-T-cell potency during bacterial infection. *Infect. Immun.* **74**, 6387–6397 (2006).

59. C. Gerlach *et al.*, The chemokine receptor CX3CR1 defines three antigen-experienced CD8 T cell subsets with distinct roles in immune surveillance and homeostasis. *Immunity* **45**, 1270–1284 (2016).

60. M. Battegay *et al.*, Quantification of lymphocytic choriomeningitis virus with an immunological focus assay in 24- or 96-well plates. *J. Virol. Methods* **33**, 191–198 (1991).

61. J. Antonchuk, G. Sauvageau, R. K. Humphries, HOXB4 overexpression mediates very rapid stem cell regeneration and competitive hematopoietic repopulation. *Exp. Hematol.* **29**, 1125–1134 (2001).

62. V. Ostiguy, E.-L. Allard, M. Marquis, J. Leignadier, N. Labrecque, IL-21 promotes T lymphocyte survival by activating the phosphatidylinositol-3 kinase signaling cascade. *J. Leukoc. Biol.* **82**, 645–656 (2007).

63. M.-H. Lacombe, M.-P. Hardy, J. Rooney, N. Labrecque, IL-7 receptor expression levels do not identify CD8+ memory T lymphocyte precursors following peptide immunization. *J. Immunol.* **175**, 4400–4407 (2005).

64. J. Chaix *et al.*, Cutting edge: CXCR4 is critical for CD8+ memory T cell homeostatic self-renewal but not rechallenge self-renewal. *J. Immunol.* **193**, 1013–1016 (2014).

65. A. M. Bolger, M. Lohse, B. Usadel, Trimmomatic: A flexible trimmer for Illumina sequence data. *Bioinformatics* **30**, 2114–2120 (2014).

66. A. Dobin *et al.*, STAR: Ultrafast universal RNA-seq aligner. *Bioinformatics* **29**, 15–21 (2013).

67. B. Li, C. N. Dewey, RSEM: Accurate transcript quantification from RNA-seq data with or without a reference genome. *BMC Bioinformatics* **12**, 323 (2011).

68. M. I. Love, W. Huber, S. Anders, Moderated estimation of fold change and dispersion for RNA-seq data with DESeq2. *Genome Biol.* **15**, 550 (2014).

69. M. E. Pipkin, M. G. Lichtenheld, A reliable method to display authentic DNase I hypersensitive sites at long-ranges in single-copy genes from large genomes. *Nucleic Acids Res.* **34**, e34 (2006).

70. J. D. Buenrostro, P. G. Giresi, L. C. Zaba, H. Y. Chang, W. J. Greenleaf, Transposition of native chromatin for fast and sensitive epigenomic profiling of open chromatin, DNA-binding proteins and nucleosome position. *Nat. Methods* **10**, 1213–1218 (2013).

71. M. Lohse *et al.*, RobiNA: A user-friendly, integrated software solution for RNA-seq-based transcriptomics. *Nucleic Acids Res.* **40**, W622-7 (2012).

72. B. Langmead, S. L. Salzberg, Fast gapped-read alignment with Bowtie 2. *Nat. Methods* **9**, 357–359 (2012).

73. F. Ramírez *et al.*, deepTools2: a next generation web server for deep-sequencing data analysis. *Nucleic Acids Res.* **44**, W160-5 (2016).

74. Y. Zhang *et al.*, Model-based analysis of ChIP-seq (MACS). *Genome Biol.* **9**, R137 (2008).

75. S. Anders, W. Huber, Differential expression analysis for sequence count data. *Genome Biol.* **11**, R106 (2010).

76. L. Odagiu, N. Labrecque, Early programming of CD8+ T cell response by the orphan nuclear receptor NR4A3. Gene expression omnibus (GEO). https://www.ncbi.nlm.nih.gov/geo/query/acc.cgi?acc=GSE143513. Deposited 13 January 2020.